Oriented Half Gaussian Kernels and Anisotropic Diffusion

Baptiste Magnier and Philippe Montesinos

Ecole des Mines d'ALES, LGI2P, Parc Scientifique G. Besse, 30035 Nîmes Cedex, France

Keywords: Half Anisotropic Gaussian Kernel, Diffusion PDEs.

Abstract: Nonlinear PDEs (partial differential equations) offer a convenient formal framework for image regularization and are at the origin of several efficient algorithms. In this paper, we present a new approach which is based (i) on a set of half Gaussian kernel filters, and (ii) a nonlinear anisotropic PDE diffusion. On one hand, half Gaussian kernels provide oriented filters whose flexibility enables to detect edges with great accuracy. On the other hand, a nonlinear anisotropic diffusion scheme offers a means to smooth images while preserving fine structures or details, e.g. lines, corners and junctions. Based on the calculus of the gradient magnitude and two diffusion directions, we construct a diffusion control function able to achieve precise image regularization. Some quantified experimental results compared to existing PDEs approaches and a discussion about the parameterizing of the method are presented.

1 A FRAMEWORK OF ANISOTROPIC DIFFUSION WITH PDE

Obtain regularized versions of noisy, corrupted or degraded images caused for example by compression artifacts is a difficult task in image processing. However, preserving significant internal structures is a field that has largely benefited from techniques of Partial Differential Equations (PDE) (Aubert and Kornprobst, 2006; Magnier and Montesinos, 2013). PDEs belong to one of the most important part of mathematical analysis and are closely related to the physical world. In this context, images are considered as evolving functions of time and a regularized image can be seen as a version of the original image at a special stage. Thereby, PDEs methods smooth locally the image following one or several directions which are different in each point of the image. In this paper, let us note $I : \Omega \to \mathbb{R}$, $(\Omega \subset \mathbb{R}^2)$ a grey level image with $I(x,y)$ corresponding to the pixel intensity of coordinates (x,y). Considering I_0 the original image, the general evolution model can be formally written in the following form:

$$\begin{cases} \frac{\partial I}{\partial t}(x,y,t) & = & F(I(x,y,t)) \\ I(x,y,0) & = & I_0(x,y) \end{cases} \quad (1)$$

where F is a given image processing algorithm, preserving edges having high gradient. F represents a function of the original image I_0 and its first and second order spatial derivatives (Caselles and Morel, 1998).

It should be noted that Koenderink (Koenderink, 1984) was the first to underline the equivalence between the convolution with a Gaussian kernel of standard deviation $\sqrt{2t}$ and the solution of the PDE describing the heat diffusion, at a time t. This smoothing process, called isotropic diffusion, is known to smooth noise but blur edges, leading to loose image structures. In order to regularize images by controlling the diffusion, Perona and Malik (Perona and Malik, 1990) have proposed a model described by the following equation:

$$\frac{\partial I}{\partial t}(x,y,t) = \operatorname{div}(g(\|\nabla I\|) \cdot \|\nabla I\|) \quad (2)$$

where div represents the divergence operator and $g(s) : [0, +\infty[\to]0, +\infty[$ a decreasing function satisfying $g(0) = 1$ and $g(+\infty) = 0$, this function could be chosen as $g(\|\nabla I\|) = e^{\left(-\frac{\|\nabla I\|}{K}\right)^2}$, with $K \in \mathbb{R}$ a constant that can be assimilated to a gradient threshold or a diffusion barrier.

The decomposition of the eq. 2 with the second derivatives of I in orthogonal directions $(\xi \perp \eta)$ respectively in the edge direction called ξ and in the gradient direction labelled $\eta = \frac{\nabla I}{\|\nabla I\|}$ enables to understand the diffusion behavior (Kornprobst et al., 1997):

$$\frac{\partial I}{\partial t}(x,y,t) = c_\xi \cdot I_{\xi\xi} + c_\eta \cdot I_{\eta\eta} \quad (3)$$

where $(I_{\xi\xi}, I_{\eta\eta}) = \left(\frac{\partial^2 I}{\partial \xi^2}, \frac{\partial^2 I}{\partial \eta^2}\right)$, c_ξ and c_η are coefficients tuning the diffusion (diagrammed in Fig. 1(a)). When $c_{\xi\xi} = c_{\eta\eta} = 1$, the eq. 3 is equivalent to the heat equation (Koenderink, 1984). Choosing $c_\xi = g(\|\nabla I\|)$, a gradient function and $c_\eta = g(\|\nabla I\|) + \|\nabla I\| \cdot g'(\|\nabla I\|)$, the diffusion process described in eq. 3 can be interpreted as two directional heat flows[1] with different diffusion intensities in the η and ξ directions to preserve discontinuities:

- Inside homogeneous regions, the gradient magnitude $\|\nabla I\|$ is small and the diffusion becomes isotropic.

- On edges, the diffusion becomes anisotropic, being attenuated by the function g, and is inhibited when the two coefficients $(c_{\xi\xi}, c_{\eta\eta})$ tend to zero.

Diffusion control is done with finite differences so that many contours of details are preserved. However, within images corrupted by a heavy noise, generally, this noise is not totally removed because the diffusion process is inhibited.

Gaussian filtering for gradient estimation has been used in a number of works to elaborate the model presented in eq. 3 less sensitive to noise and more stable. We can mention here the approach of Alvarez et al. (Alvarez et al., 1992) which induces for each pixel either an adaptive unidirectional tangential diffusion $I_{\xi\xi}$ at level of edges or an efficient isotropic smoothing for noise removal inside homogeneous regions. Nevertheless, this smoothing model does not allow a progressive diffusion in the gradient direction η because it depends on two diffusion barriers. Consequently, in the presence of a high noise, even in homogeneous regions, this diffusion scheme behaves like the *Mean Curvature Motion* (Catté et al., 1992) (MCM) method which consists in performing the diffusion only along the tangential direction ξ or along isophote lines. Although the *MCM* scheme regularizes the image in edge directions, this approach tends to round corners after a certain number of iterations and can create stripes inside noisy homogeneous regions.

Instead of considering only the gradient magnitude to drive the diffusion, tensorial approaches (Weickert, 1999; Tschumperlé and Deriche, 2005; Tschumperlé, 2006) contribute to another image diffusion formalism. From a structure tensor $J_\rho = G_\rho * \nabla I_\sigma \nabla I_\sigma^T$, where G_ρ denotes a Gaussian kernel of standard deviation ρ, authors of (Weickert, 1999; Tschumperlé and Deriche, 2005; Tschumperlé,

---

[1] Note that if $\|\nabla I\| > \frac{K}{\sqrt{2}}$, then $c_\eta < 0$ and the diffusion equation behaves locally like an inverse diffusion equation which is an unstable process enhancing features.
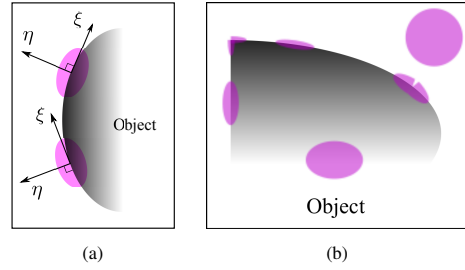

Figure 1: Diagrams of edge diffusion. (a) An image contour and its moving vector basis (ξ, η) and diffusion representation with ellipsoids. The more the gradient is high, the more the ellipse is elongated. Gradient and tangential direction denoted (η, ξ) and diffusion representation with ellipsoids, note that ellipsoids are not always oriented in the ξ direction using tensorial methods. (b) Our desired diffusion representation with half ellipsoids, the more the edge is sharped and the angle is acute, the more the half ellipses are thin.

2006) elaborate a tensor field which specifies the local smoothing geometry defined from the spectral elements of the structure tensor. Then, using the *divergence* (Weickert, 1999) or the *trace* (Tschumperlé and Deriche, 2005), the smoothing along a contour in inversely proportional to the contour strength in the direction of the eigenvector associated to the higher eigenvalue. Inside homogeneous regions, eigenvalues are close to zero and the diffusion becomes isotropic.

As demonstrated in (Tschumperlé and Deriche, 2005), *trace* based PDE is best suited to understand the local smoothing geometry behavior and these diffusion scheme ensure coherence smoothing directions but the Gaussian behavior on curved structures or corners results in a "mean curvature flow effect" leading to round small structures or corners. In order to compensate this drawback, the author of (Tschumperlé, 2006) proposed a curvature-preserving smoothing PDE that diffuses the image I along a field of vectors **w** issued by the eigenvectors of J_ρ. Despite the fact that the author of this method (Tschumperlé, 2006) has demonstrated that it better preserves corners and small details in the image, as the other tensorial approaches, when the anisotropic coefficient is too large, the diffusion of a high noise brings a fiber effect in homogeneous regions. To avoid this undesired diffusion effect, it is preferable to use a higher standard deviation of the Gaussian σ, however this leads to delocate even so the corners, diffuse small objects and also blur edges.

In this paper, we propose a new PDE scheme that regularizes images considering two contour directions. This diffusion process correctly preserves corners as well as small objects and becomes isotropic inside homogeneous regions without generating un-

desired fiber effect of artifacts. Thanks to a rotating Gaussian derivative half-filter, we extract a gradient amplitude and determine two edge directions. As illustrated in Fig. 1(b), if the gradient magnitude is small, the two major smoothing directions are straightened for an opposite alignment (i.e. 180°), becoming thereby either tangential to the edge or creating an isotropic diffusion inside flat regions. Then we apply an anisotropic diffusion on each pixel using new control functions adapted to our objectives of image regularization.

2 ORIENTED HALF GAUSSIAN KERNELS

Steerable filters (Freeman and Adelson, 1991; Jacob and Unser, 2004) or anisotropic edge detectors (Perona, 1992) perform well in detecting large linear structures (see kernels in Fig. 2 (a) and (b)). Close to corners however, the gradient magnitude decreases as the edge information under the scope of the filter decreases. Consequently, the robustness to noise concerning small objects becomes very weak.

A simple solution to bypass these effects would be to consider paths crossing each pixel in several directions. Wedge steerable filters introduced by Simoncelli and Farid (Simoncelli and Farid, 1996) are composed of asymmetric masks providing orientation of edges in different directions issued from a pixel. Akin to oriented histograms, the *saliency* of the gradient measure is calculated at each of discretized orientations (a wedge filter is presented in in Fig. 2 (d)). An advantage of these oriented filters is that they allow a characterization of junctions (Mühlich et al., 2012). In (Michelet et al., 2007) is presented also an asymmetric operator based on a sliding rectangular window where the orientation is defined as being the angle that corresponds to the maximum homogeneity i.e. the minimum variance. Unlike the Gaussian function, which is an optimal solution for the Canny criteria (Canny, 1986), in the direction of the edges, these oriented filters have a constant amplitude on almost the whole extent of the mask.
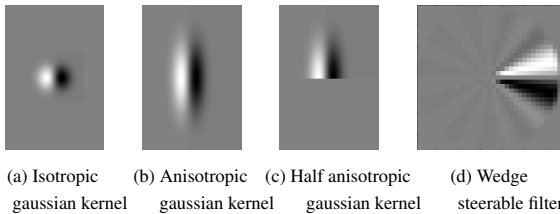
(a) Isotropic gaussian kernel   (b) Anisotropic gaussian kernel   (c) Half anisotropic gaussian kernel   (d) Wedge steerable filter

Figure 2: Different 2D derivative Gaussian kernels and a wedge filter.

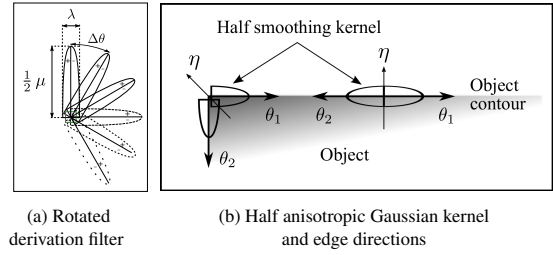(a) Rotated derivation filter   (b) Half anisotropic Gaussian kernel and edge directions

Figure 3: A thin rotating Gaussian derivative half-filter.

The idea developed in (Montesinos and Magnier, 2010) was to "cut" the derivative (and smoothing) Gaussian kernel in two parts: a first part along an initial direction, and a second part along a second direction (Figs. 2(c) and 3). At each pixel of coordinates (x,y), a derivation filter is applied to obtain a derivative information called $Q(x,y,\theta)$:

$$Q(x,y,\theta) = I_\theta * C_1 \cdot H(-y) \cdot x \cdot e^{-\left(\frac{x^2}{2\lambda^2} + \frac{y^2}{2\mu^2}\right)} \quad (4)$$

where I_θ corresponds to a rotated image[2] of orientation θ, C_1 is a normalization coefficient, (x,y) are pixel coordinates, and (μ,λ) the standard deviations of the anisotropic Gaussian filter. Since we only require the causal part of this filter along Y axis, we simply "cut" the smoothing kernel by the middle, in an operation that corresponds to the Heaviside function H. $Q(x,y,\theta)$ represents the slope of a line derived from a pixel in the perpendicular direction to θ.

To obtain gradient magnitude measure $\|\nabla I\|$ and its associated direction η on each pixel P, we first compute the global extrema of the function $Q(x,y,\theta)$, with θ_1 and θ_2. θ_1 and θ_2 define a curve crossing the pixel (an incoming and outgoing direction). Two of these global extrema are combined to obtain $\|\nabla I\|$:

$$\begin{cases} \|\nabla I\| &= \max_{\theta \in [0,360[} Q(x,y,\theta) - \min_{\theta \in [0,360[} Q(x,y,\theta) \\ \theta_1 &= \arg\max_{\theta \in [0,360[}(Q(x,y,\theta)) \\ \theta_2 &= \arg\min_{\theta \in [0,360[}(Q(x,y,\theta)) \end{cases}$$

$$(5)$$

Once $\|\nabla I\|$, θ_1 and θ_2 have been obtained, the edges can be easily extracted by computing local maxima of $\|\nabla I\|$ in the direction of the angle $\eta = (\theta_1 + \theta_2)/2$

---

[2] As explained in (Montesinos and Magnier, 2010), the image is oriented instead of the filter (like the oriented filter presented in (Michelet et al., 2007)) so as to decrease algorithmic complexity and to allow use of a recursive Gaussian filter (Deriche, 1992). As a matter of fact, for implementation purpose we replace the filtering of the initial image I_0 by a filter oriented along the varying direction θ with the filtering of an image I_θ, rotated by an angle $-\theta$, by the constant filter of orientation 0. This last operation is described by eq. (1) and is completely equivalent to a rotated filtering.
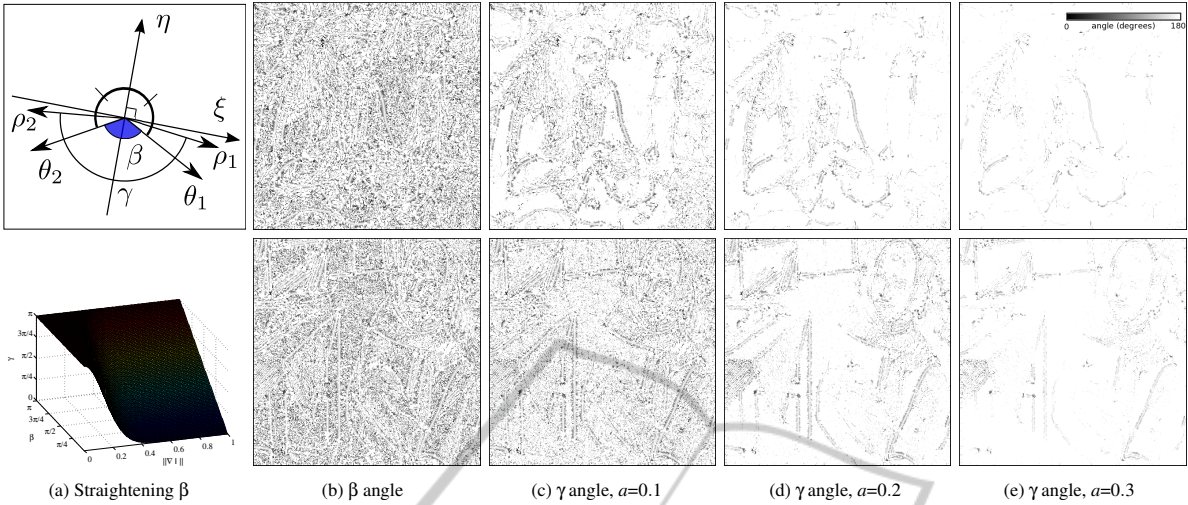
(a) Straightening β   (b) β angle   (c) γ angle, *a*=0.1   (d) γ angle, *a*=0.2   (e) γ angle, *a*=0.3

Figure 4: Different angles representation, the straightening up function and γ angle representation for corrupted images in Figs. 8(b) and 9(b) in function of different values of *a*. The more the image must be regularized, the more the *a* parameter must be large (e.g. *a* = 0.2 for a heavy noise, see bottom). *The more the pixel value is dark, the more the ange is acute.*

followed by an hysteresis threshold (see (Montesinos and Magnier, 2010) for further details). In this paper, we are solely interested in the gradient magnitude and the two directions (θ_1, θ_2) which are improved (see next section) to be used in our diffusion scheme discussed in Section 3.2.

Due to their adjustable lengths, rotating filters enable computing two precise diffusion orientations in the edge directions, even at high noise levels. More details about the effect of noise can be found in (Magnier et al., 2011a) where the authors have evaluated this edge detector as a function of noise level, and, a comparison with other approaches (Perona, 1992) shows the efficiency of this method. Note that these kernels have been used in several diffusion schemes in image regularization (Magnier et al., 2011b; Magnier et al., 2012; Magnier et al., 2013a; Magnier et al., 2013b; Magnier and Montesinos, 2013).

3 SMOOTHING IN TWO EDGE DIRECTIONS

3.1 Two Improved Edge Directions in a Diffusion Sceme

As detailed in Section 1, PDE-based image regularization techniques using gradient intensities or tensorial diffusion smooth the image either in the orthogonal directions (ξ, η), or in the directions provided by the eigenvectors of the structure tensor. However, both approaches do not take into account the two ac-

tual directions of edges, for example at a corner level.

For removing texture and preserving edges, issued by an edge classifier, the original idea developed in (Magnier et al., 2011b) was to smooth the image in the two contour directions called (ξ_1, ξ_2): $\frac{\partial I}{\partial t}(x, y, t) = I_{\xi_1\xi_2} = \frac{\partial^2 I}{\partial \xi_1 \partial \xi_2}$. As textures are annihilated, this approach is not adapted for image regularization, especially because the diffusion is not controlled.

In (Magnier et al., 2013b), a pixel classification determines roughly if a pixel belongs to a homogenous region or an edge, then, authors have developed a new diffusion method. Inside edge regions, a function of the gradient magnitude issued by half Gaussian kernels (eq. 5) and also of the angle between the two diffusion directions (θ_1, θ_2) called $\beta = abs(\theta_1 - \theta_2)$ (Fig. 4(a)) drives the diffusion process:

$$\frac{\partial I}{\partial t}(x, y, t) = \frac{e^{-\left(\frac{\|\nabla I\|}{K_1}\right)^2} + e^{-\left(\frac{(\pi - \beta)}{(\pi \cdot K_2)}\right)^2}}{2} \cdot \frac{\partial^2 I}{\partial \theta_1 \partial \theta_2}, \quad (6)$$

with $K_{i, i \in \{1,2\}} \in]0; 1]$. This diffusion process combines isotropic and anisotropic diffusion, while preserving the edges and corners of different objects in highly noisy images. Nevertheless, instead of enhance textures, authors use of the heat equation, smoothing them isotropically. Moreover, as the anisotropic diffusion process is applied only at position of edges, it creates undesired lineaments near edges caused by the directional diffusion (θ_1, θ_2).

The anisotropic edge detector based on half kernels informs (eq. 5) both on the importance of the contours (gradient value) and its directions (θ_1, θ_2). Our regularization method uses these two orientations in the smoothing process in function of the angle β

| (a) Lena original | (b) Our method | (c) Enlargement of (a) | (d) Enlargement of (b) |

Figure 6: Our algorithm applied on a real image polluted by an acquisition noise.

(a) Function $e^{-\left(\frac{(\pi-\gamma)}{(\pi\cdot k)}\right)^2}$ (b) f_k function, $k = 0.6$
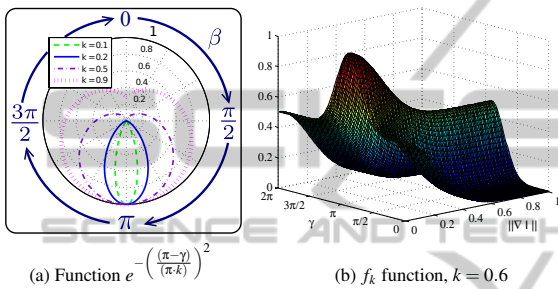
Figure 5: Control functions of the diffusion process.

3.2 An Approach Preserving Contours and Smoothing Regions

between θ_1 and θ_2. However, inside homogeneous regions, due to the level lines on the image surface, θ_1 and θ_2 are not opposite directions (i.e. $\beta \neq \pi$, see Fig. 6(c)), thus the diffusion does not perform isotropically. Here, we propose to align the orientations diffusion when the gradient value is low (i.e. $\theta_1 = \theta_2 + \pi$). To achieve this, a new angle called γ between the two edges directions is defined as:

$$\gamma = \min(\beta + \pi \cdot e^{-\frac{\|\nabla I\|}{a^2}} - \pi \cdot e^{-\frac{1}{a^2}}, \pi) \qquad (7)$$

The more $\|\nabla I\|$ is close to zero, the more γ is close to π (plotted in Fig. 4(a) bottom). The parameter $a \in \,]0,1]$ steers the straightening, as shown in Fig. 4, the more a is growing, the more γ is close to π for each pixel. Now, as illustrated in Fig. 4(a), we consider the two new diffusion directions ρ_1 and ρ_2 in our method (see Section 3.2), estimated modulo 2π in function of the following table:

$\theta_1 > \theta_2$	$\theta_1 < \theta_2$
$\rho_1 = \theta_1 + \frac{\gamma - \beta}{2}$	$\rho_1 = \theta_1 - \frac{\gamma - \beta}{2}$
$\rho_2 = \theta_2 - \frac{\gamma - \beta}{2}$	$\rho_2 = \theta_2 + \frac{\gamma - \beta}{2}$

3.2 An Approach Preserving Contours and Smoothing Regions

Our algorithm enables a smoothing in the improved directions of the contours, thus preserving edges and

details ($I_{\rho_1\rho_2}$ term) while diffusing also in the direction of η for edges having a low gradient or inside homogeneous regions ($I_{\eta\eta}$ term). Furthermore, these three directions smoothing terms have to be controlled in order to preserve image contours and not to create undesired artifacts or fiber effect elsewhere. In this respect, we adapt a new PDE developed in (Magnier and Montesinos, 2013), involving the gradient magnitude (eq. 5) and the γ angle (eq. 7) driving both the diffusion terms $I_{\rho_1\rho_2}$ and $I_{\eta\eta}$:

$$\begin{cases} \frac{\partial I}{\partial t}(x,y,t) &= f_k \cdot (I_{\rho_1\rho_2} + f_h \cdot I_{\eta\eta}) \\[2mm] f_k &= \dfrac{e^{-\left(\frac{\|\nabla I\|}{k}\right)^2} + e^{-\left(\frac{(\pi-\gamma)}{(\pi\cdot k)}\right)^2}}{2} \\[2mm] f_h &= e^{-\left(\frac{\|\nabla I\|}{h}\right)^2}, \text{with } (k,h) \in \,]0;1]^2 \end{cases}$$
$$(8)$$

The f_k function ensures the diffusion preserving edges and corners whereas the f_h function enables a permanent smoothing in the gradient direction for noisy homogeneous regions. One one hand, the more the h value is close to 1, the more edges are blurred, one the other hand the more the k value is close to 1, the more the diffusion process is important. Contrary to (Alvarez et al., 1992), these control functions are not threshold functions but continuous functions (Fig. 5). Thus, the diffusion is never only in the (ρ_1, ρ_2) directions. In case of a small gradient and a γ angle close to π, the considered pixel will be widely diffused (see Fig. 5(a)). If the gradient absolute value is large and the γ angle is small, smoothing is weak and operates mainly along these two orientations (ρ_1, ρ_2).

4 EXPERIMENTAL RESULTS AND ANALYSIS

In this section, we present several results of our regularization method compared to different other PDEs
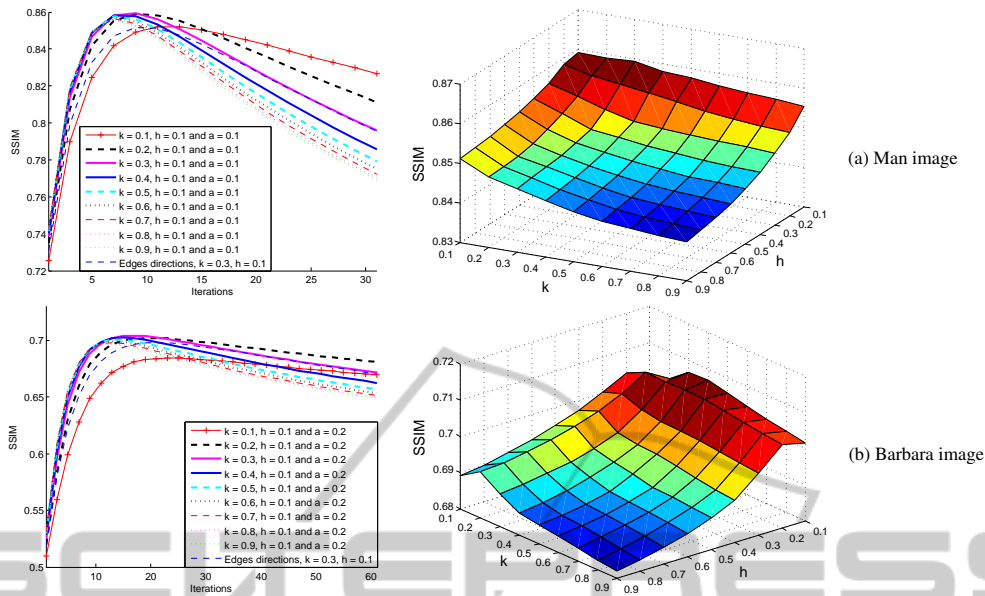
Figure 7: SSIM evolution in function of the (k, h) parameters. On the right: highest score.

approaches. For each result, presented below, we detail the parameters used either for our algorithm, or for other methods. Also, we show a SSIM (Wang et al., 2004) evaluation of noisy images as a function of the number of iterations using different parameters, which permits us to discuss about the choice of the best parameters couple (k, h). Note that, in order to obtain precise diffusion directions (θ_1, θ_2), we use a discretization angle of $\Delta\theta = \frac{\pi}{90} = 2°$ and the standard deviation of the half anisotropic Gaussian are $\mu = 5$, $\lambda = 1$ for the gradient extraction (eq. 5).

Firstly, the image in Fig. 6(a) is corrupted by a low acquisition noise because it is a scan of the original Lena from Playboy. After 10 iterations, our method removes this noise, and plain regions become totally homogeneous whereas small objects are well preserved (see details in Fig. 6(b)). Diffusion parameters are $(k, h) = (0.3, 0.1)$ and $a = 0.1$ because the noise is low in this image.

The second image shown in Fig. 8(b) is a natural image contaminated by a Gaussian noise ($\sigma = 10$). We aim to regularize this picture and preserve edges as far as possible. As presented in Fig. 8(g), (h) and (i), comparing the absolute error between the original image and the regularized image, our algorithm preserves better edges than tensorial results (Tschumperlé and Deriche, 2005; Tschumperlé, 2006). To obtain a better visualization, note that the absolute error images are corrected following a curve on the image histogram, as presented in Fig. 8(c). This visualization process is the same for each absolute error image presented in this paper.

The third noisy image presented in Fig. 9(b) contains a random Gaussian noise of standard deviation $\sigma = 20$. Due to this high noise and the texture, this image is particularly difficult to regularize correctly while preserving the thin texture. For each filter, we choose the parameters that gives the best results. In order to obtain comparative results, we choose the same width (i.e. standard deviation) of the Gaussian kernel for approaches using this function (i. e. $\sigma = \mu = 1$ for (Alvarez et al., 1992; Weickert, 1999; Tschumperlé and Deriche, 2005; Tschumperlé, 2006)). We compare our result with the *MCM* (Catté et al., 1992), the methods of Perona-Malik (Perona and Malik, 1990), Alvarez et al. (Alvarez et al., 1992), tensorial driven diffusion (Weickert, 1999; Tschumperlé and Deriche, 2005; Tschumperlé, 2006) and Magnier et al. (Magnier et al., 2013b).

It is easy to remark that *MCM* and Perona-Malik models do not remove correctly the noise. Algorithm of Alvarez et al. loses the texture and creates artifacts at position of edges. Tensors (Weickert, 1999; Tschumperlé, 2006) diffusion creates a fiber effect in homogeneous regions due to the high noise. Tensorial result of Tschumperlé (Tschumperlé and Deriche, 2005) gives a good result even if this method is known to distort corners but creates a graininess effect inside homogeneous regions (see details in Fig. 9(l)). Our algorithm restores correctly edges (Fig. 9(i)), does not create undesirable fiber effect inside homogeneous regions and enables a regularization of stripes textures with the use of thin half kernels (details in Fig. 9(m)).

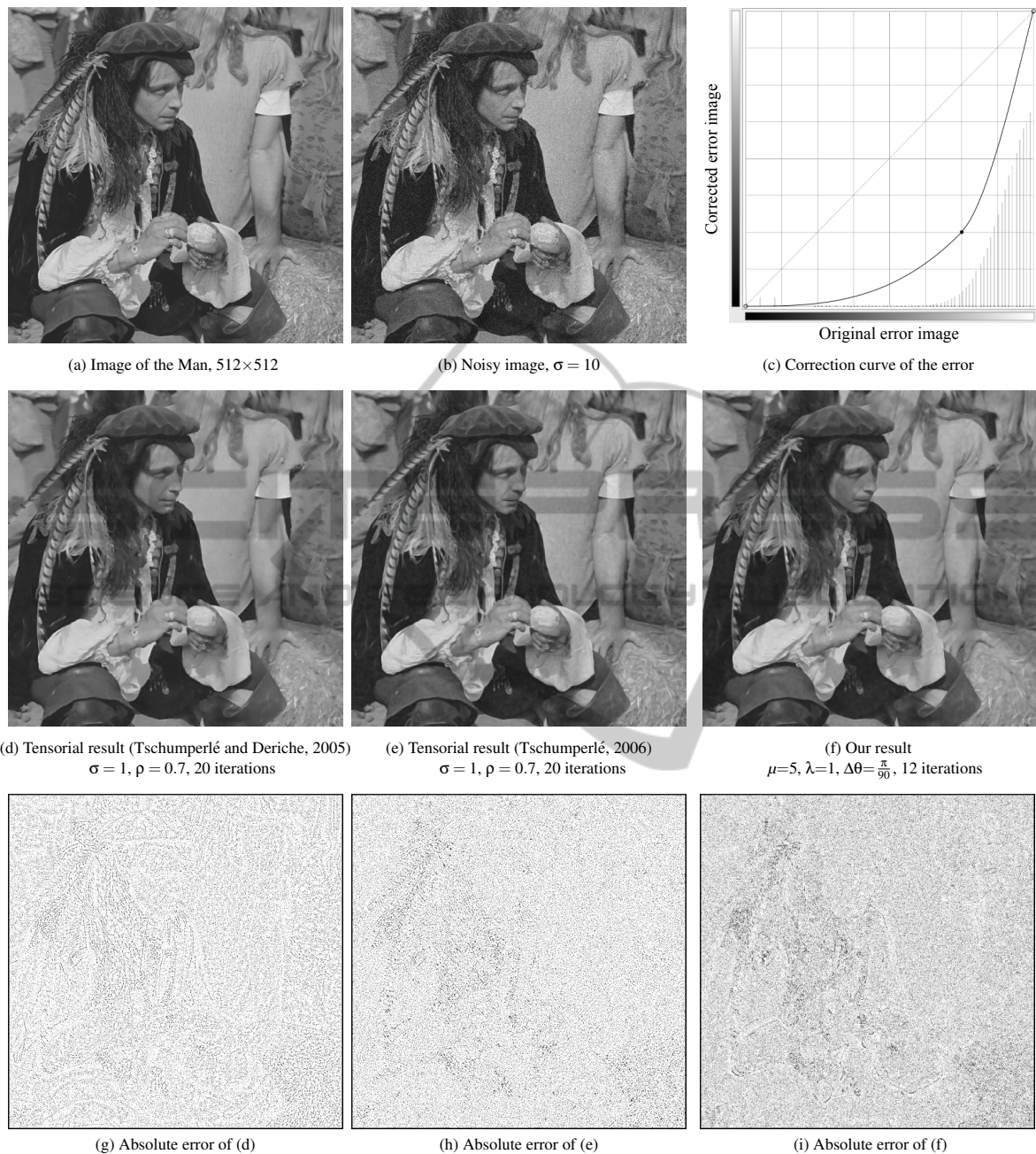We have tested different values of the couple (k, h)

(a) Image of the Man, 512×512

(b) Noisy image, $\sigma = 10$

(c) Correction curve of the error

(d) Tensorial result (Tschumperlé and Deriche, 2005)
$\sigma = 1$, $\rho = 0.7$, 20 iterations

(e) Tensorial result (Tschumperlé, 2006)
$\sigma = 1$, $\rho = 0.7$, 20 iterations

(f) Our result
$\mu = 5$, $\lambda = 1$, $\Delta\theta = \frac{\pi}{90}$, 12 iterations

(g) Absolute error of (d)

(h) Absolute error of (e)

(i) Absolute error of (f)

Figure 8: Image regularization and absolute error. Absolute error are negative images.

and when $k < h$, the diffusion results in blurring edges. When $k \leqslant 0.2$, flat regions become totally homogeneous but the smoothing process is so weak on edges that they are not retored. Fig. 7 enables a better visualization for the choices of the couple (k, h) in function of the SSIM evolution. It determines that for $(k, h) = (0.3, 0.1)$, the results are the best with this set of parameters, only the a parameter (Fig. 4) and the standard deviations of the half kernels must be set in function of the image type. Generally, the choice of our half kernel filters parameters (μ, λ) has to be done in function of the noise level. In order to preserve small objects, we can choose for the length of our filter $\mu = 5$. However, the width which corresponds to the derivation filter depends on the noise level and the image size. typically, we can choose $\lambda = 1$, it enables to keep precisely edges but if the noise is higher, we can choose a larger value.

(a) Image of Barbara
512×512

(b) Degraded image with a
Gaussian noise: σ = 20

(c) Perona-Malik diffusion (Perona and Malik, 1990)
$K = 0.05$, 100 iterations

(d) Alvarez et al. diffusion (Alvarez et al., 1992)
$\sigma = 1$, 20 iterations, $K = 0.02$

(e) *MCM* diffusion (Catté et al., 1992)
20 iterations

(f) Weickert's result (Weickert, 1999)
$\sigma = 1$, $\rho = 0.7$, 50 iterations

(g) Tensorial result (Tschumperlé and Deriche, 2005)
$\sigma = 1$, $\rho = 0.7$, 20 iterations

(h) Tensorial result (Tschumperlé, 2006)
$\sigma = 1$, $\rho = 0.7$, 20 iterations

(i) Our result, k=0.3, h=0.1,
μ=5, λ=1, 20 iterations

(j) Close up in (a)

(k) Close up in (b)

(l) Close up in (g)

(m) Close up in (i)

Figure 9: Enhancement of Barbara image by different PDE methods.

5 CONCLUSIONS

In this paper, we have presented a new regularization technique based on half Gaussian filtering followed by an anisotropic PDE diffusion. This method complements previous works by calculating new directions of diffusion for a more accurate regularization of images. We have shown that the fine assessment of the diffusion direction is a key factor, and we have proposed a set of control parameters which provide very good results in restoration of noisy images. Eventually, as these diffusion directions preserve precisely corners and small objects in images, future works will focus on the extraction of corners only using the improved edges directions formula detailed in this paper.

REFERENCES

Alvarez, L., Lions, P.-L., and Morel, J.-M. (1992). Image selective smoothing and edge detection by nonlinear diffusion, ii. *SIAM J. of Num. Anal.*, 29(3):845–866.

Aubert, G. and Kornprobst, P. (2006). *Mathematical problems in image processing: partial differential equations and the calculus of variations (second edition)*, volume 147. Springer-Verlag.

Canny, F. (1986). A computational approach to edge detection. *IEEE TPAMI*, 8(6):679–698.

Caselles, V. and Morel, J. (1998). Introduction to the special issue on partial differential equations and geometry-driven diffusion in image processing and analysis. *IEEE TIP*, 7(3):269–273.

Catté, F., Lions, P., Morel, J., and Coll, T. (1992). Image selective smoothing and edge detection by nonlinear diffusion. *SIAM J. of Num. Anal.*, pages 182–193.

Deriche, R. (1992). Recursively implementing the gaussian and its derivatives. In *ICIP*, pages 263–267.

Freeman, W. T. and Adelson, E. H. (1991). The design and use of steerable filters. *IEEE TPAMI*, 13:891–906.

Jacob, M. and Unser, M. (2004). Design of steerable filters for feature detection using canny-like criteria. *IEEE TPAMI*, 26(8):1007–1019.

Koenderink, J. (1984). The structure of images. *Biological cybernetics*, 50(5):363–370.

Kornprobst, P., Deriche, R., and Aubert, G. (1997). Nonlinear operators in image restoration. In *ICVPR*, pages 325–331.

Magnier, B., Huanyu, X., Montesinos, P., et al. (2013a). Half gaussian kernels based shock filter for image deblurring and regularization. In *VISAPP*, volume 1, pages 51–60.

Magnier, B. and Montesinos, P. (2013). Evolution of image regularization with pdes toward a new anisotropic smoothing based on half kernels. In *IS&T/SPIE Electronic Imaging*, pages 86550M–86550M. International Society for Optics and Photonics.

Magnier, B., Montesinos, P., and Diep, D. (2011a). Fast Anisotropic Edge Detection Using Gamma Correction in Color Images. In *IEEE 7th ISPA*, pages 212–217.

Magnier, B., Montesinos, P., and Diep, D. (2011b). Texture Removal in Color Images by Anisotropic Diffusion. In *VISAPP*, pages 40–50.

Magnier, B., Montesinos, P., and Diep, D. (2012). A new region-based pde for perceptual image restoration. In *VISAPP*, pages 56–65.

Magnier, B., Montesinos, P., Diep, D., et al. (2013b). Perceptual color image smoothing via a new region-based pde scheme. *Electronic Letters on Computer Vision and Image Analysis 12 (1)*, 1:17–32.

Michelet, F., Da Costa, J.-P., Lavialle, O., Berthoumieu, Y., Baylou, P., and Germain, C. (2007). Estimating local multiple orientations. *Sig. Proc.*, 87(7):1655–1669.

Montesinos, P. and Magnier, B. (2010). A New Perceptual Edge Detector in Color Images. In *ACIVS*, volume 2, pages 209–220.

Mühlich, M., Friedrich, D., and Aach, T. (2012). Design and implementation of multisteerable matched filters. *TPAMI*, 34(2):279–291.

Perona, P. (1992). Steerable-scalable kernels for edge detection and junction analysis. *IMAVIS*, 10(10):663–672.

Perona, P. and Malik, J. (1990). Scale-space and edge detection using anisotropic diffusion. *IEEE TPAMI*, 12:629–639.

Simoncelli, E. and Farid, H. (1996). Steerable wedge filters for local orientation analysis. *IEEE TIP*, 5(9):1377–1382.

Tschumperlé, D. (2006). Fast anisotropic smoothing of multi-valued images using curvature-preserving PDE's. *IJCV*, 68(1):65–82.

Tschumperlé, D. and Deriche, R. (2005). Vector-valued image regularization with pdes: A common framework for different applications. *IEEE TPAMI*, pages 506–517.

Wang, Z., Bovik, A., Sheikh, H., and Simoncelli, E. (2004). Image quality assessment: From error visibility to structural similarity. *IEEE TIP*, 13(4):600–612.

Weickert, J. (1999). Coherence-enhancing diffusion filtering. *IJCV*, 31(2):111–127.